

Computer Simulation of Load Equivalence Factors

W. J. KENIS AND C. M. COBB

AASHTO's load equivalence factors are evaluated with the aid of a computational model for predicting flexible pavement response. First, the VESYS 5 computer program was verified to assure that it could be used to conduct computer road tests. Following this, damage produced by steering axles at the AASHO Road Test was evaluated in an effort to quantify the error in the AASHTO equivalence factors, because steering axles were neglected in the development of these equivalencies. Next, the computer model was used in the conduct of computer road tests with the goal of developing equivalence factors for conditions not present at the AASHO road test site. Finally, exponential relationships relating pavement deflections and strains to load equivalencies based on cracking and rutting were developed.

Traffic volume, vehicle weight, speed, tire pressure, axle spacing, and vehicle suspension are factors that must be considered when studying pavement response. Added to these are environmental conditions that constantly change, inflicting damage to the pavement. Material properties of flexible pavements, for example, are influenced not only by temperature, but also by vehicle speed. Thus, it is tempting for the pavement engineer to make simplifying assumptions in pavement design, reducing the number of variables to those that significantly affect pavement response. One such simplifying assumption involves the concept of the equivalent single axle load (ESAL) and load equivalence factor (LEF). It allows the design engineer to reduce the numerous vehicles traveling on the road to an equivalent number of single axles. The concept was first developed from the AASHO Road Test results and has been in common use since.

Because the data from the AASHO site are limited to the conditions at the site, it is desirable to investigate those factors not studied at the site; because the cost of conducting similar road tests is prohibitive, it becomes economically justifiable to use computational pavement response models. For example, tridem axle configurations, now common on the nation's highways, were not included in the AASHO Road Test traffic. Other factors not studied include axle spacings, vehicle spacings, transverse positions of the vehicles on the pavements, truck speed, and tire pressures. In addition, steering axles were neglected in the development of load equivalence factors (except for vehicles having just two single axles).

This paper includes the results of the following research objectives.

- Calibrate the VESYS 5 program to simulate the response measured at the AASHO Road test.
- Evaluate pavement response caused by steering axles in the AASHO Road Test experiments.
- Calculate LEFs based on serviceability and damage.
- Evaluate relationships between primary response LEFs and damage-based LEFs.

EQUIVALENCY CONCEPTS

At the AASHO Road Test site a number of identical thickness designs were used in various loops so that a single design was independently subjected to several different traffic loadings. Ten different vehicle types (Figure 1) were used in the test. Only one vehicle type was used in each lane so that each pavement section was subjected to only one type of loading. The distribution of vehicles was such that axle load applications accumulated at the same rate in all traffic lanes throughout the test period. Except when road conditions were prohibitive because of pavement distress or weather conditions, the vehicles traveled at a constant speed of 35 mph (1).

The primary objective of the AASHO Road Test was to establish relationships between pavement performance and design characteristics such as layer thicknesses and loading parameters. The LEFs developed as a result of the AASHO Road Test were calculated from performance equations based on the relationship between the number of load repetitions and the present serviceability of the pavement. A standard single-axle load of 18 kips was adopted. The AASHTO LEF for criteria based on present serviceability index (PSI) is

$$LEF_{PSI} = W_0/W_x|_{PSI} \quad (1)$$

where W_0 is the number of standard single axles to a limiting value of PSI and W_x is the number of any axle (single or tandem) of load x to the same limiting value of PSI. It may also be expressed in terms of the AASHTO performance equation as

$$LEF_{PSI} = \{(Lx + L_2)/(18 + 1)\}^{4.79} L_2^{-4.33} g^{(1/\beta)18 - 1/\beta x} \quad (2)$$

where L_x is the load on any single or tandem axle, β is a function of L_x plus the structural capacity of the pavement, g is a function of the ratio of the serviceability indexes and $L_2 = 1, 2$ the axle code for single or tandem axles, respectively (2). With the exception of two-axle trucks, the steering

W. J. Kenis, FHWA, HNR 20, 6300 Georgetown Pike, McLean, Va. 22101. C. M. Cobb, Department of Civil Engineering, Louisiana Tech University, Ruston, La. 71272.











Loop	Lane		Weight in Kips		
			Front	Load	Gross
2	1		2	2	4
	2		2	6	8
3	1		4	12	28
	2		6	24	54
4	1		6	18	42
	2		9	32	73
5	1		6	22.4	51
	2		9	40	89
6	1		9	30	69
	2		12	48	108

FIGURE 1 AASHO trucks (1).

axles of the vehicles were not considered to be load axles and no provision was made in the road test analyses to study the significance of the steering axles on pavement performance. Later, Scala (3) suggested that the steering axles at AASHO contributed only about 3 percent of the total damage caused by the test vehicles. However, he also suggested that for some vehicles traveling on today's highways, the steering axle carries a greater portion of the load than those used in the AASHO Road Test and may therefore contribute significantly to the total damage.

Previously, the AASHTO Design Guide included equivalencies for only single-axle loads up to 40 kips and tandem-axle loads to 48 kips. The latest AASHTO Design Guide, published in 1986, includes equivalencies for single-axle loads to 50 kips, tandems to 90 kips, and tridem to 90 kips. To obtain these new equivalencies, Equation 2 was used. For tridems, the axle code in Equation 2 was given the value of three. There is some uncertainty as to the validity of extending these equations to generate equivalencies for loads and axles not applied at the road test.

It was observed by Scala (3) that the AASHTO equivalence factors expressed by Equation 1 are approximately equal to the fourth power of the ratio of the actual loads:

$$LEF_{PSI} = (L_x/L_0)^4 \quad (3)$$

This relationship is commonly known as the Fourth Power Law where L_0 takes on the standard values 18, 30, and 40.7 for single-tandem and tridem-axle loads.

In addition to present serviceability, other pavement response measures might be used as a basis for determining load equivalence factors. For damage-based criteria (D)

$$LEF_D = W_0/W_x|_D \quad (4)$$

where W_0 and W_x are evaluated at a limiting value of distress rather than PSI, and LEF_D is known as a damage equivalence factor. If one makes certain linearity assumptions on the flexible pavement fatigue cracking damage equation,

$$W|_c = K1(1/e)^{K2} \quad (5)$$

where $K1$ and $K2$ are fatigue material property constants and W is evaluated at some limiting measure of cracking, then on substitution into Equation 4 for the respective loads, the following primary response strain equivalence equation is obtained:

$$LEF_e = (e_x/e_0)^{K2} \quad (6)$$

In this equation, e is the tensile strain (primary response) for the respective loads at the bottom of the AC layer. Similarly, an expression for primary response deflection equivalency may be developed by using the rut depth equation

$$RD = d_x \mu_R W^{\alpha_R} \quad (7)$$

where d_x is pavement maximum surface deflection and μ_R and α_R are pavement system permanent deformation properties. Equation 4 may be used in Equation 7 to yield

$$LEF_d = (d_x/d_0)^{1/\alpha_R} \quad (8)$$

Canadian research regressed rebound deflection (d) against number of load repetitions to limiting PSI (4) to obtain

$$LEF_{PSI} = (d_x/d_0)^b \quad (9)$$

where b is the regression coefficient from various field experiments. Because Equations 6, 8, and 9 are functions of strain or deflection, they are called primary response equivalencies. We can solve for the exponent in any of Equations 6, 8, or 9; however, it is more enlightening to develop a general expression

$$Q = \log LEF_j / \log (PR_x / PR_0) \quad (10)$$

where Q is the exponent $1/\alpha_R$, b , or $K2$; PR is the deflection or strain primary response; and j is an identifier for PSI, cracking, or rutting. This expression is awkward when the primary response ratio or the LEF is close to or equal to 1.

One other major concern with the above equivalencies is that of defining d_x or e_x for multiple-axle configurations. For instance, Canada has defined d_x in Figure 2 for multiple axles

$$LEF_d = (d_1/d_0)^{3.8} + \sum((d_{i+1} - T_i)/d_0)^{3.8} \quad (11)$$

where

d_i, T_i = peak deflection and trough of axle i for an n axle group,

$(d_{i+1} - T_i)$ = difference in magnitude between the maximum deflection recorded under each succeeding axle and the minimum residual deflection preceding the axle, and

d_0 = pavement surface deflection caused by the standard single-axle dual tire load.

A similar approach is used in VESYS 5. The primary strain or deflection response at any point in the pavement caused by multiple axles is obtained through superposition of the response at that point caused by each axle in the multiple-axle configuration. The proportional amount of peak to valley, as shown in Figure 2, determines the magnitude of the response to be used in the repeated load damage models. For example, for tandem axles the equation would be

$$\text{Response 1} = \max [d_1, d_2]$$

$$\text{Response 2} = \min [d_1, d_2] - T_1 \quad (12)$$

The algorithm generalizes readily to higher multiple-axle groups. This procedure differs from the Canadian method in that it assigns no special treatment to the lead axle in the axle group. Rather, it assumes that the greatest damage is caused by the greatest response, regardless of which axle appears to be producing that response.

VESYS COMPUTATIONAL MODEL

The evolution of the VESYS series of computational pavement models began in the mid-1970s with the development of a prototype version, VESYS 2M, a closed form three-layer viscoelastic model (5). Since the development of VESYS 2M, ten other versions have been produced (6).

Given parameters that define the pavement, environment, and loading, VESYS can predict the pavement's behavior over time. Initially, layer theory is used to calculate primary response stress, strain, and deflection under a static loading. These values are used along with traffic loading in cumulative damage models to predict cracking, rutting, and roughness. Finally, the present serviceability index is computed.

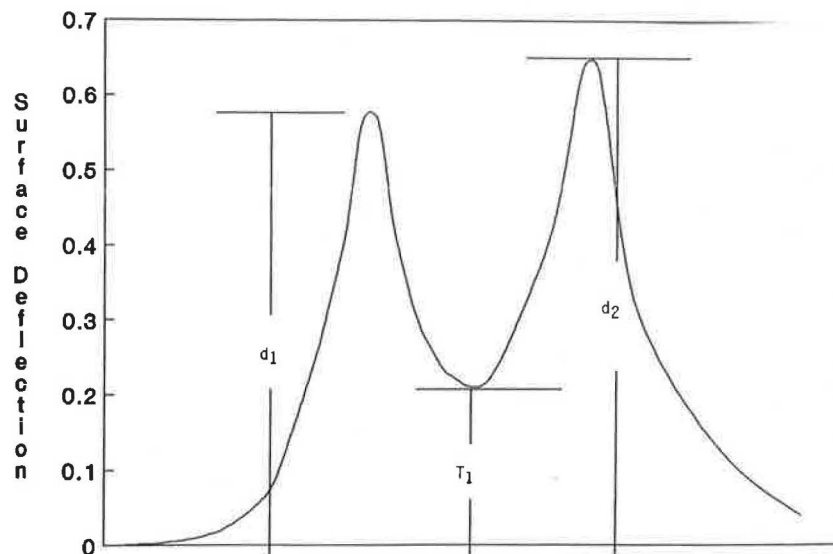


FIGURE 2 Tandem axle.

VESYS 5 has the unique feature of analyzing pavement response caused by single, tandem, or tridem axle loadings. Traffic volumes are specified in AADT (average annual daily traffic) wherein each axle group is considered to be one component of the traffic. The actual vehicle configuration may consist of several axle groups up to three axles. Each group is counted separately in the AADT designation. The user also specifies the number and length of time periods into which the traffic flow over the entire analysis period is divided. The percentage of each axle group composed in the AADT is specified and may be adjusted for seasonal variation (B. Brademeyer, unpublished FHWA data).

VERIFICATION AND CALIBRATION

Any newly developed computational pavement model must first be verified for realistic ranges of environmental, material, and traffic parameters. Once it is verified, the model can be calibrated so that predictions of pavement response are within a desirable degree of accuracy for a specific set of conditions. Calibration may be done either internally or externally (7). Internal calibration is carried out by adjusting program inputs (usually material properties). External calibration is achieved by applying a calibration factor to the program output.

Most of the mechanistic models comprising VESYS 5 and used in this study were verified and calibrated for AASHO conditions in previous studies. However, in this study VESYS 5 is further calibrated internally by comparing results of damage predictions with measured values of rutting, cracking, and serviceability from the 16 AASHO Road Test sections shown in Table 1. The sections were selected so that two thickness designs could be analyzed over the entire range of loading configurations for the main loops (3 through 6).

A study conducted by Kenis et al. (8) in 1982 developed values for layer stiffness moduli, permanent deformation properties (GNU and ALPHA), and fatigue properties K_1 and K_2 for four seasons. These values are shown in Table 2 and were applied to determine inputs for VESYS 5 for use in the calibrations.

The traffic rates applied to VESYS (for the calibrations) were kept identical to the rates applied at the AASHO test site.

Seasonal Data

VESYS 5 has the capability of modeling environmental changes at variable intervals of up to 12 seasons per year. Primary response is generated for each season. Determination of the number and length of seasons was done by analysis of deflection measurements taken at the AASHO Road Test every 2 weeks. These deflections were averaged for the 2-year period and are plotted as shown in Figure 3. The environmental change having the greatest effect on deflections is the spring thaw, beginning around March 18 and ending around May 13. Pavement temperatures for each season were obtained by adding 24°F to the average air temperature for each of five seasons, as suggested by Rauhut and Jordahl (9). It was determined from this plot that the conditions at the AASHO Road Test could adequately be modeled with the five seasonal intervals shown.

Layer Stiffness Moduli

Adjustments were made to the stiffness moduli of Table 2 so that they would correspond with the seasons selected for VESYS 5. The final values used for the study are given in Table 3. The surface layer creep compliance curve shown in Figure 4 was used along with the time temperature shift relationship (8):

$$a_T = t_T/t_{T0} \quad (13)$$

where

t_{T0} = time corresponding to the compliance at reference temperature T_0 ,

TABLE 1 MAIN DESIGNS FOR AASHO LOOPS 3 THROUGH 6

AASHO LOOP	Axle Type	Axle Load (pounds)	AASHO Section Number*	
			4-3-8 Design	4-6-9 Design
3	Single Tandem	12,000	121	139
		24,000	122	140
4	Single Tandem	18,000	589	577
		32,000	590	578
5	Single Tandem	22,400	481	455
		40,000	482	456
6	Single Tandem	30,000	269	303
		48,000	270	304

* Surface-Base-Subbase Thickness, inches

TABLE 2 MATERIAL PROPERTIES USED BY KENIS ET AL. (14)

Material Property	Winter	Spring	Summer	Fall
Modulus (KSI)				
Surface	1600	550	140	450
Base	40	30	40	40
Subbase	20	15	20	20
Subgrade	4.5	3	4.5	4.5
Permanent Deform				
Surface				
GNU	0.04	0.078	0.10	0.082
ALPHA	0.60	0.72	0.60	0.71
Base				
GNU		Variable Function of Stress		
ALPHA	0.75	0.75	0.75	0.75
Subbase				
GNU		Variable Function of Stress		
ALPHA	0.75	0.75	0.75	0.75
Subgrade				
GNU	0.04	0.15	0.04	0.04
ALPHA	0.75	0.75	0.75	0.75
Fatigue				
Surface				
K1	1.0E-13	1.8E-12	1.3E-8	3.0E-1
K2	5.10	5.01	4.87	4.99

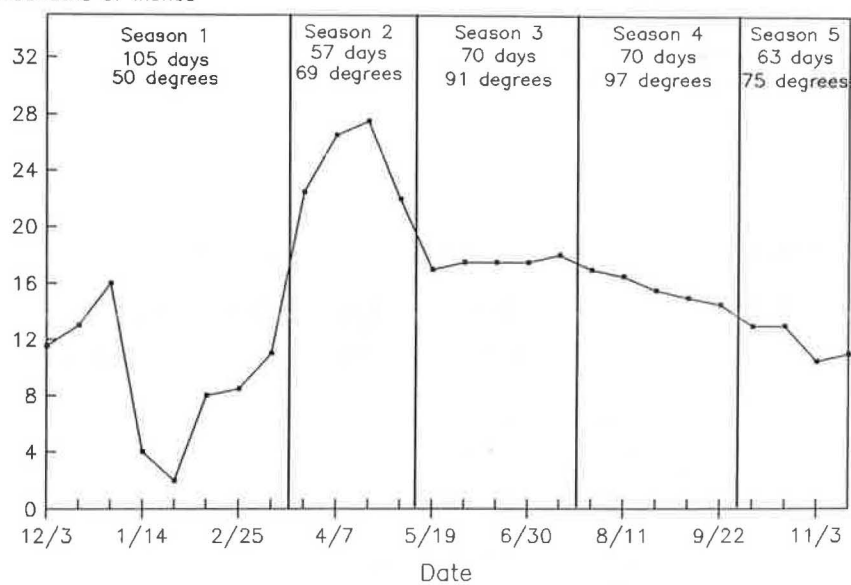
Mean Deflection
Thousandths of Inches

FIGURE 3 AASHO loop 1.

TABLE 3 SEASONAL LAYER MODULI

	Moduli (ksi) for				
	Season 1	Season 2	Season 3	Season 4	Season 5
Surface	1,600	550	170	140	460
Base	42	30	33.5	37	41
Subbase	21	15	16.5	18	21
Subgrade	4.7	3.3	3.8	4.1	4.6

NOTE: Season 1: 105 days, 50°F; season 2: 57 days, 69°F; season 3: 70 days, 91°F; season 4: 70 days, 97°F; and season 5: 63 days, 75°F.

t_T = time corresponding to the same compliance on shifted curve at temperature T , and

a_T = time temperature shift factor = $10^{(T_0 - T)\beta}$

The time t_{T_0} on the master creep compliance curve of Figure 4 for any temperature T (with t_T estimated to be 0.03) is obtained by

$$t_{T_0} = (0.03)10^{(T - T_0)\beta} \quad (14)$$

where $\beta = 0.054$ as recommended by Rauhut and Jordahl (9). To obtain the surface stiffness moduli, the compliance for each temperature is taken from the master creep compliance curve and inverted.

For the spring season, base and subbase stiffness moduli were obtained from nomographs found previously (10). Results from CBR tests (11) taken before placement of the pavement at the AASHO Road Test were used to estimate spring subgrade moduli.

For the remaining seasons, base, subbase, and subgrade stiffness moduli were obtained by adjusting the values selected for spring using several different procedures, viz., seasonal multipliers and back calculations using deflection basins measured at the AASHO Road Test (2).

Layer Permanent Deformation Properties

The results of repeated load tests conducted by the FHWA on a control mix of asphalt concrete at 40°F, 75°F, and 90°F

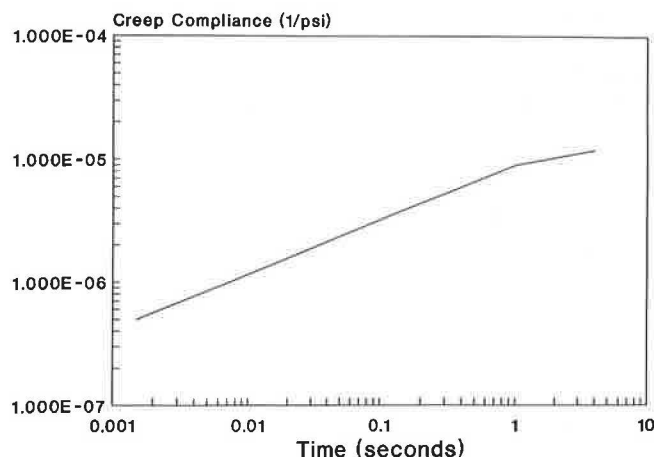


FIGURE 4 Road test surface (8).

were used to obtain values of ALPHA and GNU for the surface layer for input to VESYS 5 (8). Values of GNU for the base and subbase in the Kenis et al. study (8) were established as functions of deviator stress. However, a recent study by Leahy (unpublished FHWA data) showed that deviator stress has little influence on GNU for these layers. Preliminary runs for the current study supported Leahy's conclusion. The ALPHA values for the base and subbase, when varied, were found to have little influence on pavement response for all seasons (8).

Data from the AASHO Road Test (11) indicate that the moisture content in the subgrade was about 14 percent for the spring and 12 percent for the other seasons. The relationship between GNU and moisture content for the subgrade is plotted in Figure 5. The effect of moisture content on ALPHA for the subgrade has not been established. The initial values from the study by Kenis et al. (8) were used to make adjustments through trial and error until reasonably good predictions of rutting were obtained. Table 4 shows final values of GNU and ALPHA used in this study.

Fatigue Properties

Fatigue properties (K_1 and K_2) for the surface layer have been established at 70°F to be approximately 2.0×10^{-12} and 5.0, respectively (9). Seasonal adjustments to these values were made using adjustment factors given in the VESYS user's manual (5). Again, calibration was obtained through trial and error by comparing measured values of cracking with VESYS 5 predictions. Values of K_1 and K_2 used for the surface layer in the equivalency analysis are as follows:

	Season 1	Season 2	Season 3	Season 4	Season 5
K_1	6.0×10^{-12}	2.0×10^{-12}	1.0×10^{-10}	1.3×10^{-07}	1.0×10^{-11}
K_2	5.1	5.01	4.95	4.87	4.99

Calibration Simulations

The examples of pavement response given in Figure 6, are evidence of reasonable predictions of rutting (a), cracking (b), and serviceability for single and tandem axles (c) at AASHO. Inner and outer wheel path damage are evidence of a high

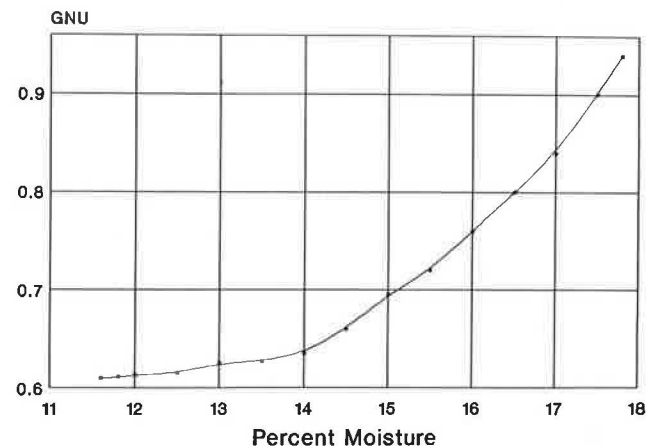


FIGURE 5 Subgrade GNU (8).

TABLE 4 SEASONAL LAYER PERMANENT DEFORMATION PROPERTIES

	GNU/ALPHA				
	Season 1	Season 2	Season 3	Season 4	Season 5
Surface	.04	.055	.10	.10	.082
	.50	.45	.72	.60	.71
Base	.045	.1	.215	.23	.15
	.75	.75	.75	.75	.75
Subbase	.01	.04	.938	.04	.015
	.75	.75	.75	.75	.75
Subgrade	.04	.05	.04	.04	.04
	.75	.50	.75	.75	.75

degree of variability as indicated in the plots. Considering that the seasonal material properties for all sections are represented by a single value, deviations from measured data are expected. It is interesting to note that the deviations between measured inner and outer wheel path often are greater than deviations between VESYS and any one of the measured values. The results of these simulations establish VESYS as a suitable tool for analysis of the main objectives of this study.

ANALYSIS

To study the main objectives, a single pavement design (corresponding to AASHO sections 121, 122, 269, and 270 of loops 3 and 6) having surface, base, and subbase thicknesses of 4, 3, and 8 in., respectively, was selected. Axle loads and tire pressures used are given in Table 4. They were selected so that the contact radii ranged from 5 to 8 in. (which also corresponds to the range for AASHO vehicles). The AASHO traffic rates were used in VESYS for the steering axle analysis; however, adjustments were made to these rates for the LEF damage and primary response analyses.

Steering Axle Analysis

To study the validity of neglecting steering axles in the development of AASHO LEFs, each of the four vehicles shown in Figure 1 for loops 3 and 6 was applied in a VESYS 5 simulation both with and without steering axles. Traffic rates identical to those at AASHO were used. An example of the resulting damage predictions is given in Figure 7 for AASHO test section 270. It is obvious from this plot that very little pavement damage was caused by the steering axles in the VESYS simulation. Simulations on the other three vehicles produced identical conclusions. For the four sections analyzed, average steering axle damage was about 2.10 percent for rutting, 0.125 percent for cracking, and 1.31 percent for serviceability. Simulation of the remaining sections at the road test should yield similar results because all of the steering axles supported approximately the same percentage of loading.

Serviceability and Damage-Based Analysis

Initial computer runs made with the AASHO traffic rates for tridem axle configurations resulted in total loss of serviceability early in the simulation, during the first spring thaw. This loss led to equivalencies for very heavy tridem axle loadings that were unexpectedly low. These equivalencies are plotted in Figure 8 and are compared with the AASHO equivalencies. Thus, traffic rates were lowered so that damage occurred at a stable rate throughout the simulation period, but the relative variability in traffic volume was maintained over the five seasons. Using the adjusted traffic rates, load equivalence factors based on VESYS 5 predictions of rutting, cracking, and serviceability were calculated for comparison with AASHO LEFs using Equation 1 for serviceability and Equation 4 for rutting and cracking. Terminal levels of $\frac{3}{4}$ in. for rutting, 50 percent for cracking, and 3.0 for serviceability were used in determining equivalencies. The calculated equivalencies are given in Figures 9 through 12.

Figures 9 and 10 compare AASHO LEFs to those based on the VESYS 5 predictions of serviceability. In general, the VESYS 5 serviceability LEFs for all axle configurations are closely correlated with AASHO LEFs. Minor deviations are apparent, suggesting that equivalencies based on VESYS 5 predictions of serviceability increase at a rate slightly lower than do AASHO equivalencies.

VESYS predictions of damage-based LEFs are plotted in Figures 11 and 12. Tridem equivalence is plotted in Figure 11 for three different damage criteria. The choice of damage criterion appears to have a mixed effect on LEF; however, rutting equivalencies are, in general, lower for all configurations. Rutting LEFs are also plotted in Figure 12 but grouped according to axle configuration instead of damage criterion (for other damage criteria, the plots are similar in shape). Figure 12 suggests the existence of a consistent relationship between equivalencies for multiple-axle configurations.

An interesting phenomenon can be observed from Figures 11 and 12. In the figures it is apparent that a wide range of axle loads have equivalencies based on rutting approximately equal to one. For these axle loads, failure occurred during

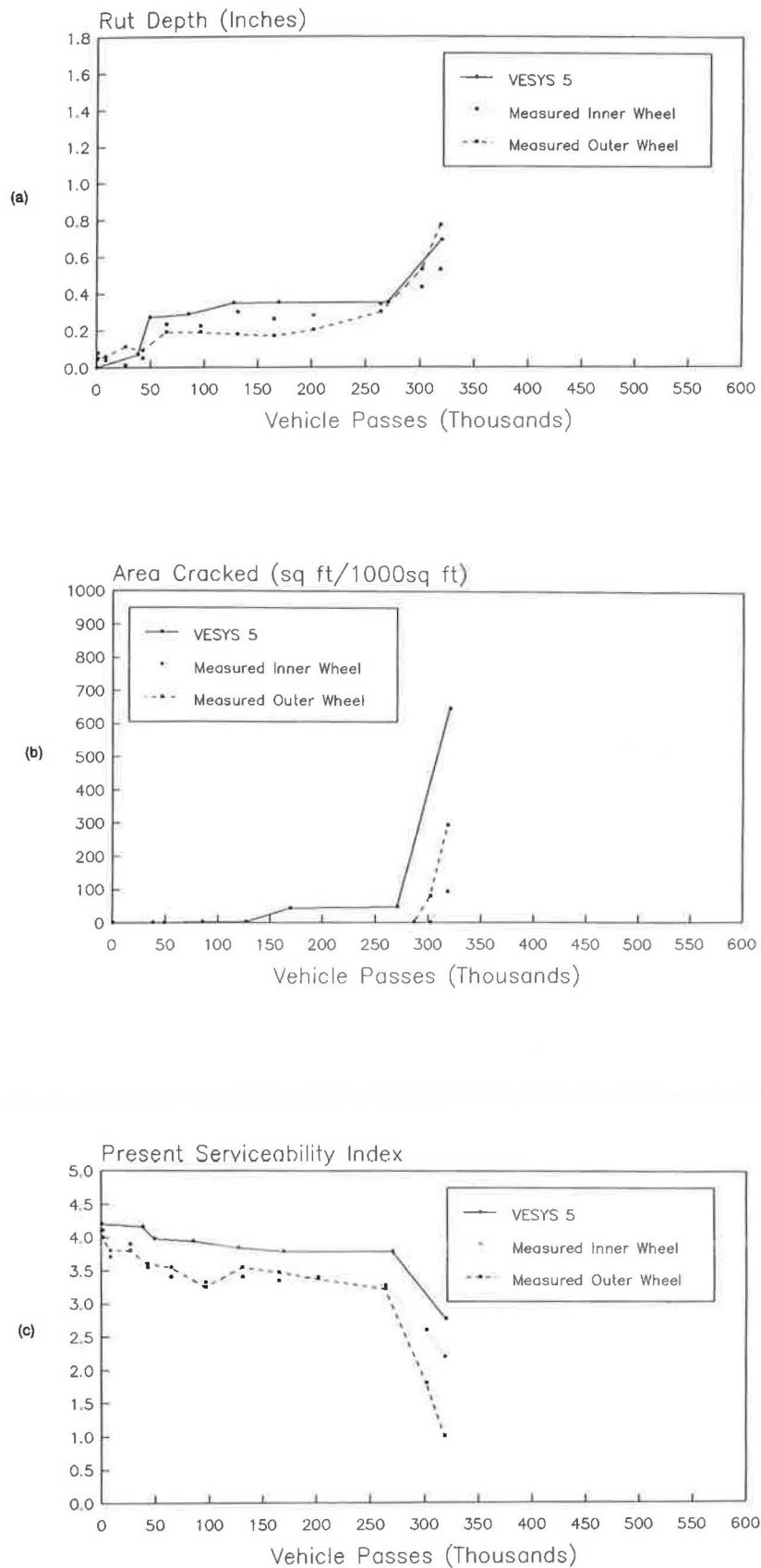


FIGURE 6 AASHO Section 121, 4-3-8 pavement 12 K single: (a) rut depth; (b) area cracked; and (c) present serviceability index.

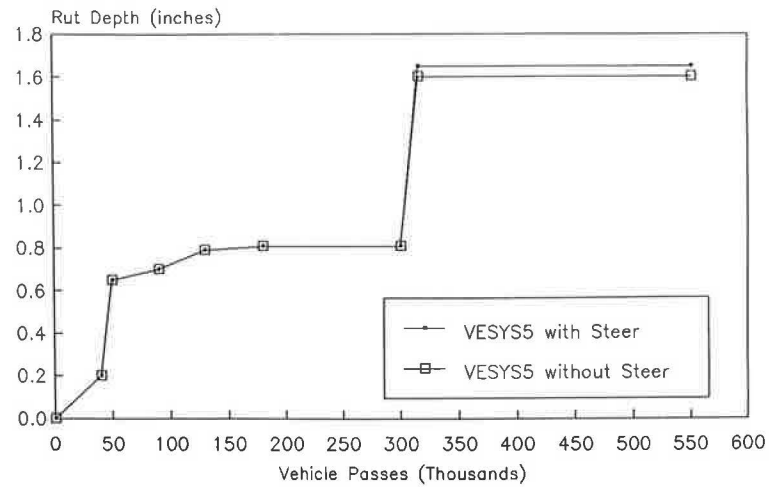


FIGURE 7 AASHO Section 270, 4-3-8 pavement 48 K tandem.

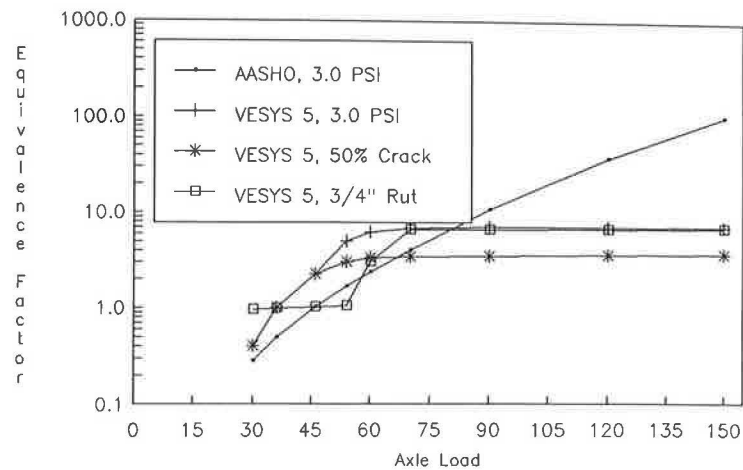


FIGURE 8 Tridem equivalence (AASHO traffic rate).

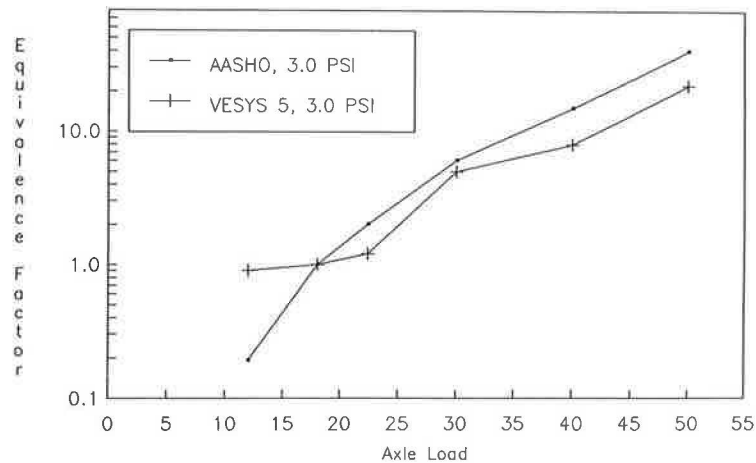


FIGURE 9 Single-axle equivalence (adjusted traffic rate).

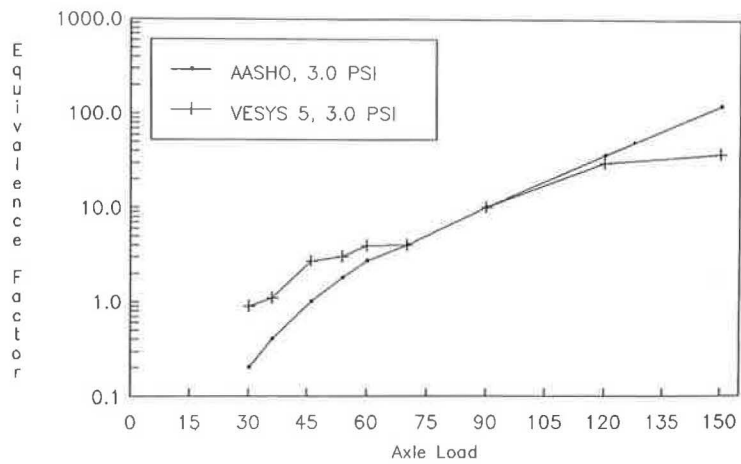


FIGURE 10 Tridem equivalence (adjusted traffic rate).

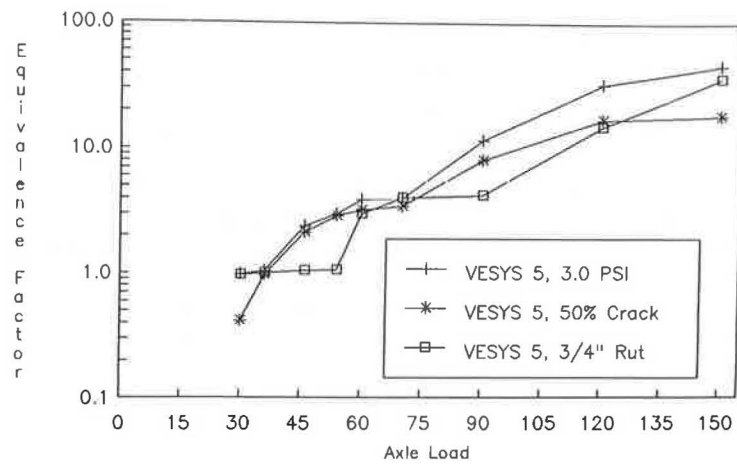


FIGURE 11 Tridem equivalence (adjusted traffic rate). VESYS predictions of damage-based LEFs.

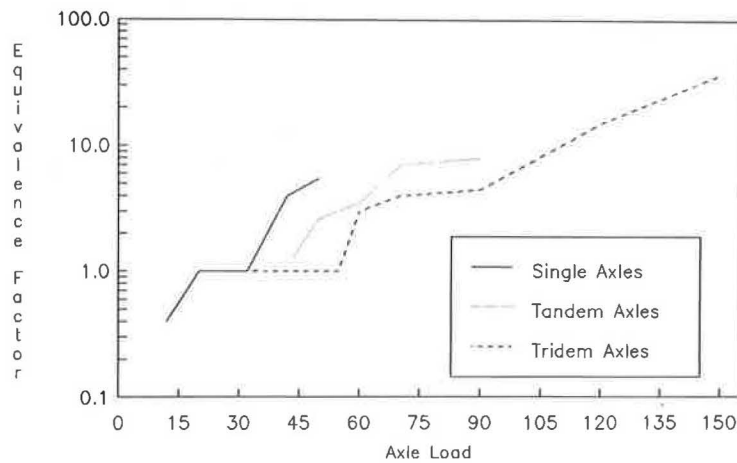


FIGURE 12 VESYS rutting equivalence (adjusted traffic rate).

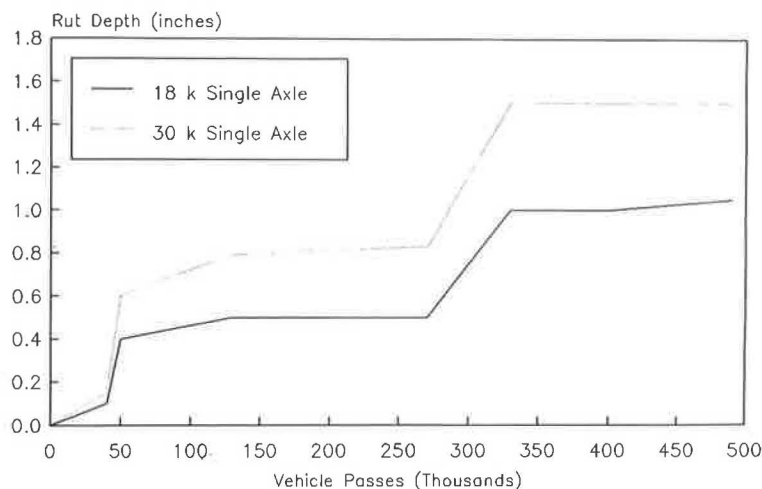


FIGURE 13 VESYS 5 rutting predictions (AASHO traffic rate).

the second spring thaw, as was the case with the 18-kip standard. The existence of this phenomenon is described in Figure 13, which shows VESYS 5 predictions of rutting for the 18-kip standard and for the 30-kip single-axle loads. The sharp increase in rutting to levels above $\frac{3}{4}$ in. occurs at approximately the same number of repetitions (250,000 to 300,000 vehicle passes) for both loads. The equivalency for the $\frac{3}{4}$ -in. failure level is 1.00, whereas the equivalency for a $\frac{1}{2}$ -in. failure level is much higher at approximately 6.00.

These examples illustrate that the season in which failure occurs (also a function of traffic rate) has an important influence on the value of the load equivalence factor. Generally, if failure occurs during the same seasons of the same year for both the standard axle load and the load for which the equivalency is being obtained, the equivalency will be close to one. If failure occurs for one of the axle loads during the following year, the equivalency will be higher for loads greater than the standard and lower for loads smaller than the standard, assuming that traffic rates are not altered. It is important to note that from the four main traffic loops at the road test, 45 percent of the sections were removed from the test before the end of

the first spring season. This percentage is broken down by load as follows:

Singles	Tandems
12 kip—77%	24 kip—87%
18 kip—50%	32 kip—47%
22.4 k—37%	40 kip—37%
30 kip—17%	48 kip—13%

The above analyses suggest that, had traffic rates been reduced so that all sections lasted throughout the test period, the AASHTO load equivalencies would have been higher for loads greater than the standard and lower for loads smaller than the standard.

Primary Response Analysis

Strain Based—The AASHTO and the cracking LEFs (Figures 9–12) were related to the strain ratios for each of the five seasons and for each of the single-, tandem-, and triple-axle loads (Table 5) using Equation 10. The exponent was then

TABLE 5 AXLE CONFIGURATIONS USED IN LOAD EQUIVALENCE ANALYSIS

Single Axles		Tandem Axles		Tridem Axles	
Load	Tire Pressure	Load	Tire Pressure	Load	Tire Pressure
12 kip	75 psi	24 kip	75 psi	30 kip	75 psi
18 kip	75 psi	32 kip	75 psi	36 kip	75 psi
22.4 kip	75 psi	40 kip	75 psi	46 kip	75 psi
30 kip	75 psi	48 kip	80 psi	54 kip	75 psi
40 kip	75 psi	60 kip	100 psi	60 kip	75 psi
50 kip	80 psi	70 kip	115 psi	70 kip	75 psi
		90 kip	135 psi	90 kip	75 psi
				120 kip	100 psi
				150 kip	135 psi

calculated for all cases. Exponents for tandem-axle cracking LEFs are plotted in Figure 14 (similar trends were observed for single and tridem). Note that the curves tend to infinity when the strain ratios are close to or equal to one. Also, when the LEF in the numerator is identically equal to one, an undefined 0/0 condition exists. Strain ratios close to one occur when the global maximum strain of the axle group approaches that strain produced by the 18k standard single-axle load. Note that the tandem exponent is a positive number at all times. This exponent is positive because the numerator of Equation 10 (log of cracking LEF) is at all times greater than the denominator (log of strain ratios). A similar set of curves (not shown) for tandems was produced using "log of AASHTO LEF" in the numerator. The exponents, although positive numbers, were generally smaller than those based on cracking simply because the AASHTO LEFs used were generally smaller than the cracking LEFs.

For singles and tridems the AASHTO LEFs generally were larger (for intermediate loads) than cracking LEFs, and thus the exponents based on AASHTO LEFs were generally larger than those based on cracking LEFs. This analysis suggests that the magnitude, the behavior, and the type of LEF used in the numerator play a significant role in the power law formulation.

Another equally important observation from Figure 14 demonstrates the sensitive nature of the power law formulation, especially for winter and summer conditions. For all axle types and for all formulations (AASHTO or cracking), the exponent at the intermediate load level is higher for the warmer seasons. This higher value is directly attributable to the magnitude of the strain ratios used in Equation 10 (the LEF in the numerator as defined for each load is an average value over all seasons). Thus the strain ratios in the warmer seasons (at intermediate load levels) are significantly smaller than the strain ratios in the colder seasons. This occurrence is a result of using linear elastic layer theory when the contact radius is increased (if contact pressure remains constant) as load is increased. Had contact pressure been increased and contact radius been held constant as load was increased, then the large differences between winter and summer strain ratios

would have been negligible. Since contact radius does, in fact, increase with increasing axle load, there is justification for developing seasonal LEFs.

Deflection Based—The exponential relationship between VESYS predictions of deflections and AASHTO LEFs was calculated similarly as for strain analysis. Tridem axle exponents for winter and summer seasons are plotted in Figure 15. Here the exponents are well-behaved, exhibiting values over all load levels between 3.5 and 4; in addition, there is little evidence of any seasonal effects on the exponents. Similar curves were obtained for single and tridems.

When rutting LEFs are used in the numerator of Equation 10, very erratic but not invalid curves are obtained. Tandem exponents are shown plotted in Figure 16. A similar reasoning as applied in the strain ratio analysis is also valid here. When the LEF in the numerator is close to one, the exponent approaches zero. This erratic behavior is solely caused by the environmentally induced stepwise behavior of the rutting LEFs shown in Figure 11. Again this illustrates the major effect that traffic rate and seasonal material property changes have on establishing levels of axle equivalency.

CONCLUSIONS AND RECOMMENDATIONS

- The good agreement between VESYS-5 predictions of rutting, cracking, and PSI with measured values at the AASHTO Road Test is justification for using VESYS to conduct extended road tests and analyses. The good agreement also justifies the internal calibration methodology applied for the calibration.
- The steering axles at the AASHTO Road Test had virtually no influence on pavement response. Therefore, the fact that they were neglected in the development of the AASHTO load equivalence factor equations is appropriate.
- The relationship between seasonal material properties and traffic rate can significantly influence load equivalence factors. To establish load equivalencies that are representative of the entire range of seasons, traffic rates should be adjusted so that damage occurs at a fairly constant rate throughout the test period. To achieve a more accurate estimation of the

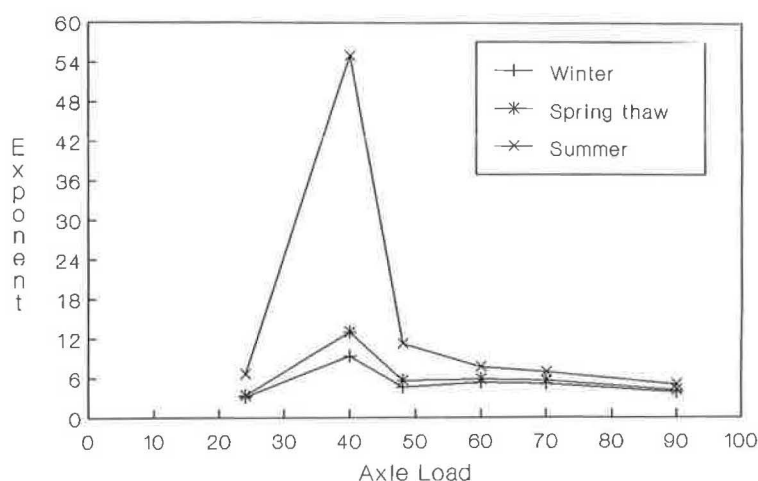


FIGURE 14 Strain-based LEF exponents: tandems (based on cracking LEF).

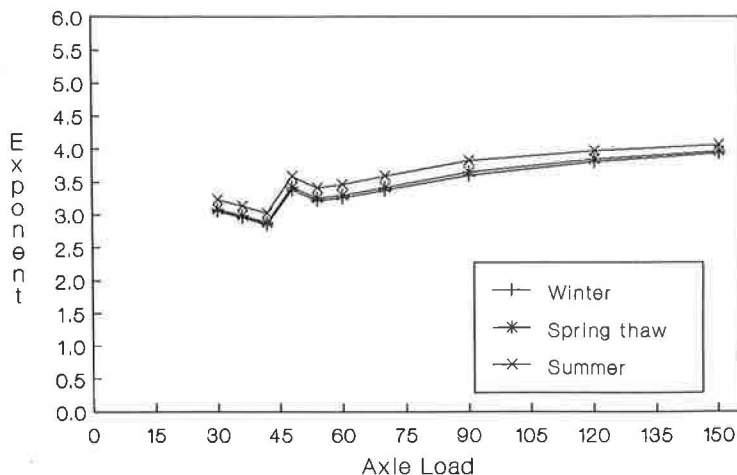


FIGURE 15 Deflect-based LEF exponents: tridems (based on AASHO LEF).

relative damage caused by various vehicle types, seasonal load equivalence factors should be considered. If traffic at the AASHO Road Test had been adjusted so that all sections lasted throughout the test period, the resulting load equivalence factors may have been different. This information is particularly important in light of the fact that the failure rate of sections subjected to lighter loads was considerably higher than the failure rate of sections subjected to heavier loads.

• Ratios of strains and deflections raised to an exponent can be used to determine load equivalence factors. The exponents based on strain vary with season; exponents based on deflection are similar for all seasons. The logarithmic power law expression is sensitive to the type, shape, and magnitude of the LEF used in the numerator.

Further study of the relative damage caused by the various vehicle types should use "computer test road" simulations to verify the

- Feasibility of using entire vehicle equivalencies,
- Effect of traffic rate on the AASHO LEF,

- Feasibility of seasonal load equivalence factors, and
- Feasibility of using primary response as a measure of vehicle damaging effects.

ACKNOWLEDGMENTS

Financial support for C. M. Cobb was provided through the National Highway Institute graduate research fellowship program. The information was condensed and edited from an FHWA unpublished report \M.S. thesis prepared by C. M. Cobb while he was a Louisiana Tech University, Ruston, Graduate Research Fellow at the Turner Fairbank Highway Research Center. Technical support for the study was provided in part by Pavements Division, FHWA, Office of Research, Development and Technology Transfer and Department of Civil Engineering, Louisiana Tech University. Special thanks are extended to Leslie K. Guice of Louisiana Tech University and to Donna Malec for her support in producing this document.

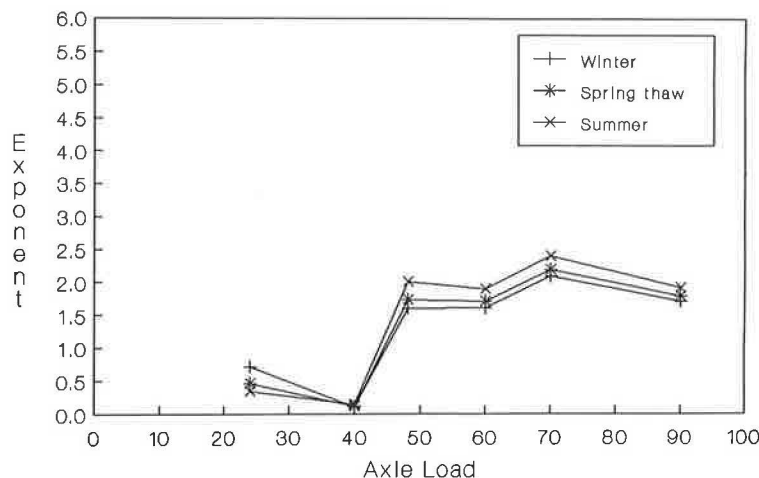


FIGURE 16 Deflect-based LEF exponents: tandems (based on rutting LEF).

REFERENCES

1. *Special Report 61A: The AASHO Road Test, History and Description of Project*. HRB, National Research Council, Washington, D.C., 1961.
2. *Special Report 61E: The AASHO Road Test, Report 5, Pavement Research*. HRB, National Research Council, Washington, D.C., 1962.
3. A. J. Scala. Comparison of the Response of Pavements to Single and Tandem Axle Loads. In *Australian Road Research Board: Proceedings of the 5th Conference*, Canberra, Ware Publishing Pty. Ltd., 1970.
4. J. T. Christison. Vehicle Weights and Dimensions Study, Vol. 8. In *Pavements Response to Heavy Vehicle Test Program, Part 2, Technical Report, Load Equivalency Factors*. Roads and Transportation Association of Canada, July 1986.
5. W. J. Kenis. *Predictive Design Procedures, VESYS Users Manual—An Interim Design Method for Flexible Pavements Using the VESYS Structural Subsystem*. Report FHWA-RD-77-154. FHWA, U.S. Department of Transportation, January 1978.
6. W. J. Kenis. The Rutting Models of VESYS. *Proc., 25th Conference on Paving and Transportation*, The University of New Mexico, Albuquerque, January 1988.
7. M. G. Sharma, W. J. Kenis, and M. Mirdamadi. Evaluation of Mechanical Parameters of In-Service Pavements from Field Data. *Proc., 6th International Conference on the Structural Design of Asphalt Pavements*, Ann Arbor, 1987.
8. W. J. Kenis, J. A. Sherwood, and T. F. McMahon. Verification and Application of the VESYS Structural Subsystem. *Proc., 5th International Conference on the Structural Design of Asphalt Pavements*, University of Michigan, Ann Arbor, and Delft University of Technology, Delft, The Netherlands, Vol. 1, August 1982.
9. J. B. Rauhut and P. R. Jordahl. Effects on Flexible Highways of Increased Legal Weights Using VESYS IIM. Report FHWA-RD-77-116, FHWA, U.S. Department of Transportation, Washington, D.C., January 1978.
10. *NCHRP Report 128: Evaluation of AASHO Interim Guides for Design of Pavement Structures*. HRB, National Research Council, Washington, D.C., 1972.
11. *Special Report 61B: The AASHO Road Test, Report 2, Materials and Construction*. TRB, National Research Council, Washington, D.C., 1962.

Publication of this paper sponsored by Committee on Flexible Pavement Design.